

Boiling a nucleus[†]

E.C. Pollacco^{1,†}, J. Brzychczyk^{1,2}, C. Volant¹, R. Legrain¹, and L. Nalpas¹

¹ CEA DAPNIA/SPhN, CE Saclay, 91191 Gif-sur-Yvette CEDEX, France

² Inst. of Phys., Jagiellonian Univ., 30-059 Krakow, Poland

D.S. Bracken, K. Kwiatkowski, K.B. Morley, E. Renshaw Foxford, V.E. Viola, and N.R. Yoder

Dept. of Chem. & IUCF, Indiana Univ., Bloomington, IN47405, USA

R.G. Korteling

Dept. of Chem., Simon Fraser Univ., Burnaby, BC, Canada

H. Breuer

Dept. of Phys., Univ. of Maryland, College Park, MD 20742, USA

J. Gomez del Campo

Oak Ridge National Laboratory, Oak Ridge, TN37831, USA

J. Cugnon

Univ. de Lige, Inst. de Physique, B-4000 Lige 1, Belgium

Recibido el 5 de febrero de 1998; aceptado el 3 de marzo de 1998

In the reaction ${}^3\text{He} + \text{Ag}$ hot nuclei are formed with excitation energies close to the total binding energy. A relatively large proportion of these events decay leaving a heavy fragment and light particles. These events have a non multifragmentation character.

Keywords: [supon]3[supoff]H₋, [supon]3[supoff]He₋, [supon]4[supoff]He, induced reactions

En la reacción ${}^3\text{He} + \text{Ag}$ se forman núcleos calientes con energía de excitación cercana a la energía de amarre total. Una proporción relativamente grande de estos eventos decae dando lugar a un fragmento pesado y partículas ligeras. Estos fragmentos poseen un carácter no multifragmentario.

Descriptores: Reacciones inducidas [supon]3[supoff]H₋, [supon]3[supoff]He₋, [supon]4[supoff]He

PACS: 25.70.Pq; 25.55.-e

1. Introduction

The study of finite nuclei under extreme conditions are under study. Acmes being exploited range from angular momentum, isospin, E^* as well low and high densities. In this paper we consider, in particular, the limits of excitation energy, E^* . This problem is an old one [1, 2] and questions whether ‘the collision lead to an explosion of the whole nucleus’. Framed in somewhat different terms, we enquire, up till what E^* can we raise a nucleus such that the probability of survival to an explosive-like process (multifragmentation) becomes small. The principle difficulty that is encountered in studies of hot nuclei is to isolate the dynamics of the heating process from the properties of hot matter itself: What would be ideal is to be able to select events with known initial mass, charge, angular momentum at normal density and with spherical shape (not to enhance a specific decay channel). From theoretical reaction mechanism studies [2–4] we believe the target can be distorted (in position and momentum space). These distortions can be attenuated though an appropriate choice of projectile and incident energy. The use of pions, anti-protons and energetic light projectiles is a step towards reaching opti-

mal conditions [5]. With new data that is becoming accessible comparative studies could be extended [2].

The use of light ions as projectiles to deposit large E^* has a number of advantages (short reaction times, no compression, small angular momentum, single source etc.) [2, 5]. However a number of difficulties related to early dynamics persist [3]. The paper by Colonna *et al.* [4] investigate this question for the system under study, ${}^3\text{He} + \text{Ag}$. Using intranuclear cascade, INC, and a stochastic one-body approach they show that for Ag target and ${}^3\text{He}$ projectile for energies up to 4.8 GeV, the nucleus is shape resilient. That is, although the nucleus is initially deformed by a moving wake, it very rapidly (≤ 60 fm/c) regains, in most cases, its original shape. From these calculations we conclude that the for the reactions at 1.8 GeV the entrance and final channel are relatively decoupled and that after a brief time the system can be represented as a hot nuclear sphere at normal density. Theoretical predictions for pre-equilibrium effects are shown to be small at this incident energy [2].

In this work the data is compared to a two step model where we couple, event-by-event, an INC calculation [6] with an evaporative code, SIMON [7]. The INC chooses randomly

the impact parameter and the calculation is stopped at 30 fm/c [4]. Each event generated by the INC code contains a single primary residue (*i.e.* before evaporation) accompanied by particle cascade (pions and nucleons). INC gives, the mass, charge, recoil velocity, angular momentum and E^* of the primary residue. At the incident energy of 1.8 GeV the E^* spectrum is Maxwellian like with a mean E^* of approximately 300 MeV. Also at 1.8 GeV, the mass spectrum is practically independent of E^* and has a mean value of 95 amu. The average angular momentum is small ($\sim 20 \hbar$). The more recent version of SIMON uses a formalism similar to that of Charity *et al.* [8]. The level density parameter employed was set at 1/13. For comparisons shown herein the generated events are filtered by the experimental angular coverage, energy thresholds and energy loss of the heavy fragments in the target. To allow a fair comparison the same operations and software conditions are applied as on the data.

2. Experimental setup

The experiment was performed at the Laboratoire National Saturne, Saclay, France, using ^3He beam at 1.8, 3.6 and 4.8 GeV. In this paper only the lower energy data set will be discussed. The target was ^{nat}Ag of thickness 1.08 mg/cm². The experimental set-up, as discussed here, consisted of three parts: (i) To detect HF a circular hodoscope, DELTA, was employed, which included 30 high field Si detectors. The target-detector flight path was approximate 60 cm and covered angles between 5 to 10°. (ii) Light charged particles, LCP, ($Z = 1$ and 2) and intermediate mass fragments, IMF, ($Z \leq 20$) were detected in an array called ISiS [9] which contains 162 triple detector telescopes in a tight geometry. Each telescope is composed of a gas ionisation chamber, IC, a fully depleted 500 m ion-implanted silicon detector and a 28 mm CsI(Tl) crystal. The geometrical acceptance is 70% and the energy thresholds were lower than 1 A.MeV. The charge, Z , resolution ranged up to 20. Mass resolution is obtained for those particles which punch through the Si counter ($Z \leq 3$). (iii) An active collimator was employed to veto the beam halo particles detected in ISiS.

3. Data analysis

The analysis of the ISiS and DELTA data consisted principally in the calibration with alpha sources, precision pulsers, time calibrators and punch through data. For ISiS this gave an overlay of practically all two-dimensional energy loss spectra ($E_{\text{IC}} \times E_{\text{Si}}$ and $E_{\text{Si}} \times E_{\text{CsI}}$). The selection of mass and charge for the LCP, and charge for the IMFs were done by drawing appropriate gates. The $E_{\text{IC}} \times E_{\text{Si}}$ have a distinct but unidentified group of particles, a fraction of which could arise from residues or fission. Including or removing events with a particle in this band does not change the results given here.

The HF mass, mass_{HF} , and velocity detected in DELTA were computed from the time between DELTA and ISiS and

energy measurements. Correction due to time delay [10] and energy defect [11] are included. The latter was achieved through a coincident set-up using slowed down fission fragments from a ^{252}Cf source in a separate measurement. Velocity and energy thresholds better than 0.3 cm/ns and 2.5 MeV respectively. We remark that in light ion induced reactions it is expected that the highest yield of HF should be for mass values close to that of the target [12]. However the mean mass detected in DELTA with a minimal bias trigger is approximately 65 amu. This is largely due to the energy loss in the target and the energy threshold in DELTA. The simulations shows that approximately 40% of the generated particles with mass in the range of 40 to 55 amu are not detected in DELTA due to the combined effects of the target and thresholds.

4. Thermal energy

As noted earlier the measurable parameters which characterise hot nuclei are apt to be perturbed by the dynamics of the heating process. The thermalisation process is very rapid (60 fm/c). Within this time the energy in the nuclear volume is thermalised through nucleon-nucleon collisions but with a net energy loss through the emission of pre-equilibrium, nucleons and composites. The angular distribution of these particles are forward peaked and their spectra extend up to the beam velocity. This fast process leaves a primary heavy fragment which subsequently generates lower energy particles. Thus the resulting kinetic energy spectra show a superimposition of the fast and slow mechanisms which for the present reaction is signalled by a change in slope with detected energy [13, 14]. To extract the primary mass, A_{th} , charge, Z_{th} and thermal energy, E_{th} , of the source for each event, only those particles with kinetic energies below given thresholds were considered. Namely, a sharp cut-off is assume. This criteria although coarse was studied using the INC+SIMON+FILTER simulator which shows a linear scaling between the *experimenta* E_{th} and the calculated energy with INC. Studies using the present data and the above criteria are given by Morley *et al.* [14]

The thermal energy of events with a minimum bias in ISiS and which included a HF (mass greater than 10amu) in DELTA were computed. The principal corrections which were introduced are the following ; (i) the detector acceptance. This includes the efficiency as a function of charge and mass for low energy particles. The efficiency corrections were established with the aid of INC + SIMON and the detector filter. (ii) By far the largest portion to the E^* is the contribution from the neutron. The mean energy per neutron K_n as a function of E_{th} was calculated using the code LILITA [15]. (iii) To obtain the total mass and charge per event, the mass of the IMFs was read off from a table of mass versus charge which takes into account the evaporation process. A similar procedure was applied to obtain the charge of the HF. The thermal quantities were calculated by summing over the particle kinetic energy, mass, charge and Q -values (Q_i) event-by-event. In this analysis the sum

was carried over heavy residue and all IMFs. For LCPs the sum was extended over particles with kinetic energies, K_i which are below 25, 32, 39, 54, and 61 MeV for p , d , t , ^3He and ^4He respectively. The thermal total charge, Z_{th} , gives the total mass, A_{th} by assuming an $Z_{\text{th}}/A_{\text{th}}$ ratio in the valley of stability. Subtracting the total detected mass from A_{th} gives the number of thermal neutrons, N_n . The thermal energy, $\epsilon^* = E_{\text{th}}/A_{\text{th}}$ was computed from the sum; $E_{\text{th}} = N_n(K_n + Q_n) + \sum(K_i + Q_i)$ over the thermal particles and corrected for the efficiencies. This analysis shows a constant $A_{\text{th}} = 92$ with E^* greater than 250 MeV which is consistent with the INC calculations. Therefore a second method was developed and adopted, where A_{th} and Z_{th} are assumed and given by the INC calculations. In this formulation the efficiency correction was not employed and the missing mass and charge and corresponding energies were assumed to arise only from LCPs in the same proportion as the detected particles in the event. Performing simulations with this procedures shows that the given by INC is well reproduced. The former method tends to give large widths in the ϵ^* observable.

Also analysed are those events where DELTA did not detect a HF. The thermal energy and mass of the residual mass is calculated using a similar algorithm as above with a fixed primary mass and correction for ISiS acceptance. The non detected particles are also assumed to arise only from LCPs in the same proportion as the detected particles in the event. Using this prescriptions for events with HF in DELTA shows that the reconstructed mass_{HF} reproduces well the measured values.

5. Results and discussion

In Fig. 1 a plot is given of the detected particles in DELTA as a function of ϵ^* imposing that the IMF multiplicity, $M_{\text{IMF}} = 0$. We note a number of features. The largest yield is for events with mass of approximately 65 amu. The island at high excitation ~ 9 A.MeV correspond to events where the HF is not detected in DELTA. The trend traced from low to high excitation is well represented by the simulation. The rectangle is drawn to have a centre at E_{th}/B corresponds to 80%. The width and height of the rectangle represent the full FWHM for the mass and ϵ^* resolution respectively. The latter value was extracted using the simulation. Releasing the condition on the M_{IMF} shows that for the window on $\epsilon^* = 6-8$ A.MeV the fraction of events with M_{IMF} greater than 0 in this region, corrected for the efficiency, is approximately 15%. These IMFs have charge distribution with a maximum at 3 and with a yield which falls rapidly with charge. This shows that the loss of mass from the HF by IMF emission for conditions in Fig. 1 is not large.

As suggested by Fig. 1, to extract higher E^* events it is favorable to consider events with low residual masses. However choosing a lower mass window raises the question of what is the lowest mass and still be able to call it a residue? Also, the HF events must have properties which are consistent with what is expected from an evaporative residue. Pro

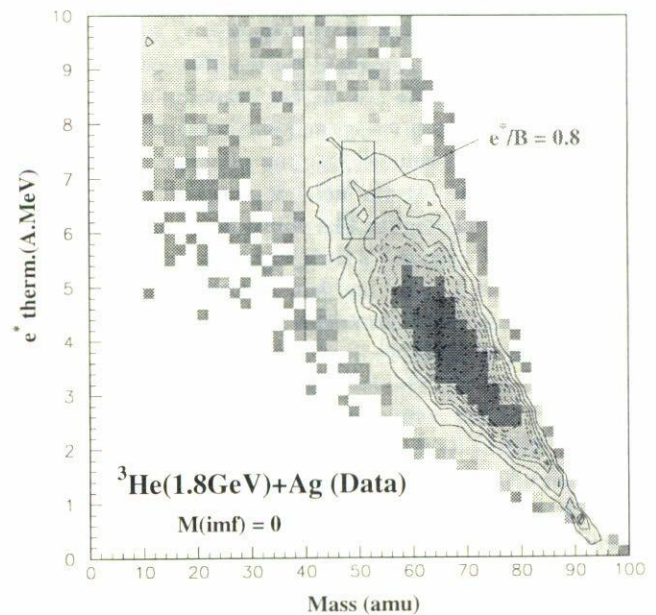


FIGURE 1. Experimental ϵ^* as a function of residual mass.

jecting out the recoil velocity spectra for the HF masses in the range of 45 to 50 amu shows that it has mean values 0.5 cm/ns, consistent with calculated values. Below this mass range (30 to 40 amu) the velocity spectrum shows a relatively flat distribution with low statistics. Therefore to consider the corresponding excitation energies we adopt a higher mass window, from 45 to 50 amu. Nevertheless, Fig. 1 (i) suggests that within statistics, the upper limit for ϵ^* is approximately 8 A.MeV as one would expect from simple considerations. Placing the adopted mass window and projecting the ϵ^* spectrum gives Fig. 2 (shaded curve). The mean value for this projection corresponds to E_{th}/B of 0.77. The dashed curve is the result of the simulation and demonstrates that the mean is well reproduced. More significantly, it shows that the width of the distribution is qualified, indicating a good understanding of the underlying processes. Comparing the extracted value of E_{th}/B with systematic from heavy ion induced reactions shows that the present result is 22% higher [16]. However it is important to add that these systematic were not performed using 4π geometrical coverage.

To obtain a measure of the probability, W_{comp} [17] for a nucleus to survive IMF emission, and therefore upper limit for multifragmentation, two formulations were employed: The first method does not include DELTA information. It assumes that at the ϵ^* being considered the vaporisation partition is negligible and that events with $M_{\text{IMF}} = 0$ and conditioned by reconstructed mass_{HF} are representative of the W_{comp} . So the number of events with ϵ^* in 5.8–6.3 A.MeV, $M_{\text{IMF}} = 0$ and with mass_{HF} greater than 30 amu is obtained. This value is normalised by the number of events, β , with the same ϵ^* range but with no restraint on M_{IMF} and mass_{HF} . After correction for the acceptance of ISiS the probability is 0.39. The second method counted the number of events in DELTA with $M_{\text{IMF}} = 0$, but using the same algorithm to cal-

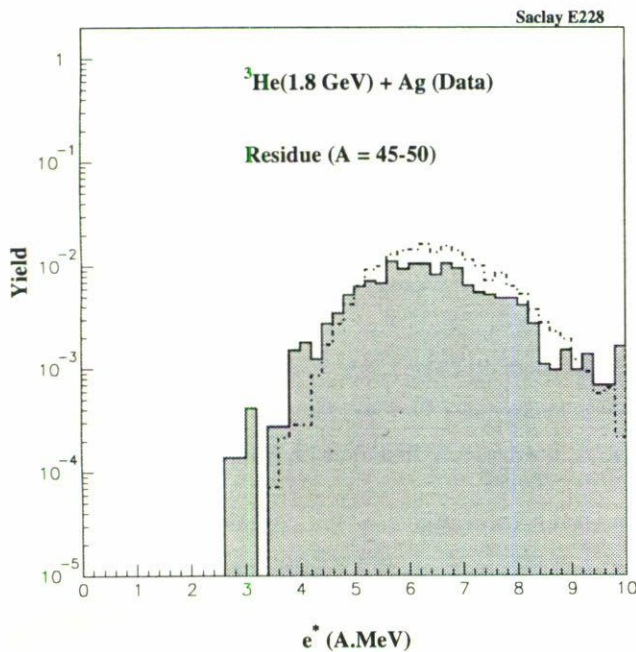


FIGURE 2. Experimental ϵ^* spectrum with the indicated mass window. The dashed curve represents the simulation.

culate ϵ^* as in the previous method and with the same ϵ^* range. This value is normalised by β for the appropriate number of recorded events and corrected for the angular distribution and target effects using the INC+EVAP+FILTER. This method gives a W_{comp} of 0.25. The difference in probabilities is attributed to the uncertainties related to the target and threshold corrections. Performing the same analysis but with $M_{\text{IMF}} = 0$ and 1 shows that the W_{comp} increase almost by a factor two. Therefore if we acknowledge that nuclei at $E_{\text{th}}/B \sim 80\%$ can evaporate an IMF we can conclude that at these excitation energies multifragmentation is not a dominant process. This result is consistent with Goldenbaum *et al.* [5] Comparing these results with those of Gross *et al.* [18] and Botvina *et al.* [2, 16] for a similar nuclei shows that the calculations underestimate the evaporative component by at least a factor of five. This is a large discrepancy.

An analysis of the 4.8 GeV data for the same system was conducted. The data shows similar trends as for the 1.8 GeV. The extraction of the W_{comp} at the same ϵ^* shows a significant decrease of approximately a factor of two. This indicates that at this incident energy a measurable distortion of the entrance channel is present. It is perhaps important to point out that at 4.8 GeV it has also been shown that a saturation in E^* occurs [13, 14].

The INC code on its own shows a good description of the data in that it reproduces the E^* saturation with incident energy [14] as well as the multiplicity in the forward angles. Further, the comparison of the data with INC+EVAP+FILTER demonstrates that the neutron, LCP

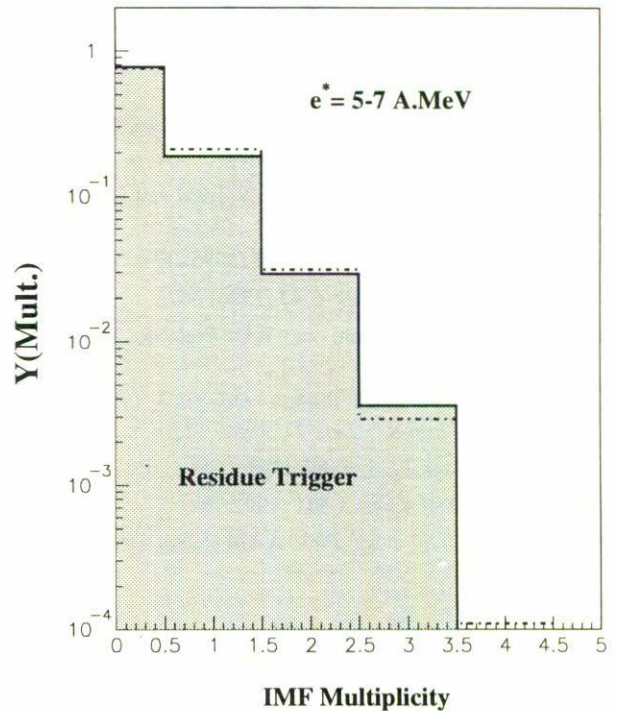


FIGURE 3. Probability for the IMF multiplicity data (solid histogram). The model predictions are given by the dashed histogram.

and IMF multiplicities (see Fig. 3) and the charged particles kinetic energy spectra are well reproduced [19]. This result proposes that the nucleon system at high E^* can still choose a sequential binary decay. However it is important to consider that the measurements correspond to averages over long disintegration chains. Therefore the comparison might not be necessarily sensitive to the alterations of the decay pattern, especially at the early stages of the process. Specifically, the present version of the INC calculations do not directly take into account the emission of composite which are present in the data.

6. Conclusions

In conclusion, we report on an experimental study of ${}^3\text{He}$ (1.8 GeV) + Ag where HF are detected at low velocity in coincidence with LCP and IMFs. The LCP and IMFs were detected in a 4 configuration with low energy threshold. Fast protons were also detected in the forward direction. On the whole the data is well described by the INC plus evaporation. Analysis is given of events at high E^* where the exit channel consist of single heavy fragment accompanied by essentially light particles. These events reach values of E_{th}/B equal to 77% with HF have masses of 47 amu. Estimates of the relative yield at this energy is at least 25% and shows that nuclei ($A \sim 100$ amu) are not easily destabilised by significant amounts of thermal energy.

- †. Experiment performed at the Laboratoire National Saturne, France.
- ‡. Present address, Pierre Sue Laboratory, CEA-CNRS, CEA/CE Saclay, 91191 Gif-sur-Yvette, France
1. N. Bohr, *Nature* **137** (1936) 344; N. Bohr and J. Wheeler, *Nature* **56** (1956) 426.
 2. J.P. Bondorf *et al.*, *Phys. Rep.* **257** (1995) 133.
 3. G. Wang *et al.*, *Phys. Rev. C* **42** (1996) 667.
 4. M. Colonna, J. Cugnon, and E.C. Pollacco, *Phys. Rev.* **55** (1997) 1404.
 5. K. Kwiatkowski, *XXXV Bormio conference*, 1997; F. Goldenbaum *et al.*, *Phys. Rev. Lett.* **77** (1986) 1230.
 6. J. Cugnon, *Nucl. Phys. A* **462** (1987) 751.
 7. D. Durand, *Nucl. Phys. A* **541** (1992) 266.
 8. R.J. Charity *et al.*, *Nucl. Phys. A* **476** (1988) 516.
 9. K. Kwiatkowski *et al.*, *Nucl. Instr. Methods A* **360** (1995) 5.
 10. H.O. Neidel and H. Henschel, *Nucl. Instr. Methods* **178** (1995) 137.
 11. S.B. Kaufman *et al.*, *Nucl. Instr. Methods* **115** (1974) 47.
 12. S.B. Kaufman and E.P. Steinberg, *Phys. Rev. C* **22** (1980) 167.
 13. E. Remshaw Foxford *et al.*, *Phys. Rev. C* **54** (1995) 749.
 14. K.B. Morley *et al.*, *Phys. Lett. B* **355** (1995) 52.
 15. J. Gomez del Campo *et al.*, *Phys. Rev. C* **41** (1991) 2689.
 16. S. Leray, *J. de Phys C* **4** (1986) 275.
 17. A. Botvina, A.S. Iljinov, and I. Mishustin, *Nucl. Phys. A* **507** (1992) 649.
 18. D.H.E. Gross, *Rep. Prog. Phys.* **53** (1990) 605.
 19. E.C. Pollacco *et al.*, *XXXV Bormio conference*, 1997.